

Expression in *Xenopus* oocytes shows that WT1 binds transcripts in vivo, with a central role for zinc finger one

Michael Lodomery^{1,*}, John Sommerville², Sarah Woolner^{1,‡}, Joan Slight¹ and Nick Hastie^{1,§}

¹MRC Human Genetics Unit, Western General Hospital, Crewe Rd, Edinburgh EH4 2XU, UK

²School of Biology, Bute Medical Buildings, University of St Andrews, St Andrews, Fife KY16 9TS, UK

*Present address: Centre for Research in Biomedicine, Faculty of Applied Sciences, University of the West of England, Coldharbour Lane, Bristol BS16 1QY, UK

‡Department of Anatomy and Developmental Biology, University College London, Gower Street, London WC1E 6BT, UK

§Author for correspondence (e-mail: nick.hastie@hgu.mrc.ac.uk)

Accepted 16 December 2002

Journal of Cell Science 116, 1539-1549 © 2003 The Company of Biologists Ltd

doi:10.1242/jcs.00324

Summary

The Wilms' tumour suppressor gene *WT1* encodes a protein involved in urogenital development and disease. The salient feature of WT1 is the presence of four 'Krüppel'-type C₂-H₂ zinc fingers in the C-terminus. Uniquely to WT1, an evolutionarily conserved alternative splicing event inserts three amino acids (KTS) between the third and fourth zinc fingers, which disrupts DNA binding. The ratio of +KTS:–KTS isoforms is crucial for normal development. Previous work has shown that WT1 (+KTS) interacts with splice factors and that WT1 zinc fingers, particularly zinc finger one, bind to RNA in vitro. In this study we investigate the role of zinc finger one and the +KTS splice in vivo by expressing tagged proteins in mammalian cells and *Xenopus* oocytes. We find that both full-length +/-KTS isoforms and deletion constructs that include zinc finger one co-sediment with ribonucleoprotein particles (RNP) on density gradients. In *Xenopus* oocytes both isoforms located to the lateral loops of lampbrush chromosomes. Strikingly, only the +KTS isoform was detected in B-snurposomes, but not when co-expressed with –KTS. However, co-expression of the C-terminus (amino

acids 233-449, +KTS) resulted in snurposome staining, which is consistent with an in vivo interaction between isoforms via the N-terminus. Expressed WT1 was also detected in the RNA-rich granular component of nucleoli and co-immunoprecipitated with oocyte transcripts. Full-length WT1 was most stably bound to transcripts, followed by the C-terminus; the least stably bound was CTΔF1 (C-terminus minus zinc finger one). Expression of the transcription factor early growth response 1 (EGR1), whose three zinc fingers correspond to WT1 zinc fingers 2-4, caused general chromosomal loop retraction and transcriptional shut-down. However, a construct in which WT1 zinc finger one was added to EGR1 mimicked the properties of WT1 (–KTS). We suggest that in evolution, WT1 has acquired the ability to interact with transcripts and splice factors because of the modification of zinc finger one and the +KTS alternative splice.

Key words: Wilms' tumour suppressor, C₂-H₂ zinc fingers, ribonucleoprotein particles (RNP), Density gradients, *Xenopus* oocytes, Lampbrush chromosomes, B-snurposomes, Nucleoli

Introduction

The Wilms' tumour suppressor gene *WT1* was first identified by positional cloning (Call et al., 1990). It is mutated in up to 15% of Wilms' tumours (Gessler et al., 1994) and 14% of acute myeloid leukaemias (King-Underwood et al., 1998). *WT1* has a key role in urogenital development and sex determination (reviewed by Little et al., 1999; Hastie, 2001). WT1 protein harbours four C-terminal C₂-H₂ zinc fingers of the 'Krüppel' type, present in the early growth response (EGR) family of transcription factors. The N-terminus of WT1 contains a Q/P-rich trans-regulatory domain, a dimerisation domain and a putative RNA recognition motif (RRM) (Kennedy et al., 1996).

Further structural complexity arises from alternative splicing. Of particular interest is an evolutionarily conserved alternative splice that inserts three amino acids (KTS) at the C-terminal end of the α -helix of zinc finger three. Structural studies have shown that the +KTS insertion severely disrupts DNA binding (Laity et al., 2000a; Laity et al., 2000b; Laity et

al., 2000c). The ratio of +KTS:–KTS isoforms is tightly controlled, and perturbations in this ratio are implicated in the aetiology of Frasier syndrome, which is characterised by severe urogenital defects, including sex reversal (Barboux et al., 1997; Klamt et al., 1998). A recent mouse model has shown that the two isoforms have distinct yet overlapping functions. By knocking out the ability of cells to make either +KTS or –KTS protein, Hammes and colleagues have shown that mutants of both strains die after birth because of kidney defects. However, mice specifically lacking the +KTS isoform (Frasier mice) show a complete XY sex reversal as occurs in the human syndrome (Hammes et al., 2001).

WT1 is a multifunctional transcription factor and several candidate target genes are known. Thus, WT1 represses the *IGFIR* gene (Werner et al., 1994), activates the *amphiregulin* (Lee et al., 1999), *bcl-2* (Mayo et al., 1999) and *SF1* genes (Wilhelm and Englert, 2002), and co-activates the *MIS* gene (Nachtigal et al., 1998). However, evidence suggests that WT1

is also involved in post-transcriptional processes. WT1 (+KTS) colocalises and co-immunoprecipitates with splice factors (Larsson et al., 1995), binds to the essential splice factor U2AF65 and associates with active splice complexes (Davies et al., 1998). WT1 also binds to WTAP (Wilms tumour associated protein) (Little et al., 2000), a nuclear protein with strong homology to the *Drosophila* protein FL(2)D. FL(2)D is required for female-specific splicing of *Sxl* and *Tra* pre-mRNAs mediated by alternative 3' splice site choice (Penalva et al., 2000). WT1 zinc fingers, both in the + and -KTS conformations, bind to RNA in vitro. In particular, zinc finger one is required for binding to GC-rich RNA derived from exon 2 of the mouse *Igf2* gene (Caricasole et al., 1996). A SELEX (in vitro selection) assay using WT1 zinc fingers resulted in the definition of three RNA aptamers (Bardeesy and Pelletier, 1998). WT1 zinc fingers bind to the RNA aptamers with dissociation constants ranging from 13.8 to 87.4 nM (Zhai et al., 2001). Consistent with its ability to bind to RNA, WT1 is present in poly(A)⁺ nuclear RNP isolated from cell lines and fetal kidneys (Ladomery et al., 1999).

The aim of this study was to search for evidence that WT1 associates with transcripts in vivo. We focused on the role of zinc finger one and the ability of +/-KTS isoforms to locate to intranuclear structures, and compared the properties of WT1 with the related transcription factor EGR1. Our approach was to express tagged constructs in mammalian cells and to exploit the many advantages of the *Xenopus* oocyte system.

Materials and Methods

Cell culture and media

African green monkey Cos7 cells were cultured in Dulbecco's modified Eagle medium (DMEM, Gibco-BRL) with 10% fetal calf serum (FCS). Mouse mesothelioma AC29 cells (Davis et al., 1992) were cultured in RPMI-1640 medium. All cell lines were cultured at 37°C with 5% CO₂.

Nuclear and whole-cell extract preparation

Medium was removed and cells rinsed with 2× ice-cold phosphate-buffered saline (PBS). Cells were scraped with a cell scraper and collected in RNase-free tubes. Cells were centrifuged for 3 minutes at 4000 rpm at 4°C, the supernatant removed, and the pellet raised in 600 µl (sufficient for each 14 mm confluent plate) of hypotonic swelling buffer (10 mM Tris-HCl, pH 7.4; 10 mM NaCl; 3 mM MgCl₂; Boehringer Mannheim protease inhibitor cocktail). Cells were left on ice for 10 minutes; 35 µl of 10% Nonidet-P40 was added to the cells, which were then mixed by short vortexing for 2 seconds and centrifuged for 1 minute at 13,000 rpm in a microfuge. When required, the supernatant (cytoplasm) was kept aside to combine with nuclear extract. The pellet (nuclei) was resuspended in an equal volume of lysis buffer (20 mM Hepes, pH 7.9; 600 mM KCl; 0.2 mM EDTA; 20 U/ml DNase I (Boehringer Mannheim), 10 U/ml Superase RNase inhibitor cocktail (Ambion) and protease inhibitor cocktail (Boehringer Mannheim). The resuspension was left on ice for 30 minutes, with mixing every 10 minutes; it was then centrifuged for 10 minutes at 13,000 rpm in a microfuge to remove insoluble material.

Transient transfection into mammalian cells

Plasmids encoding T7-tagged proteins were generated as previously described (Ladomery et al., 1999). Ten micrograms of each plasmid was transfected into Cos7 cells by electroporation (1.00 kV; 25 µF),

and into AC29 and HeLa cells using Lipofectamine (Gibco-BRL) as per manufacturer's specifications. Expression was tested by western blotting and immunofluorescence was measured using a mouse monoclonal antibody directed against the T7 epitope (Novagen). Two days after transfection, cells were fixed for 10 minutes in 1:1 acetone:methanol, and blocked in 2% BSA in PBS, 7% (v/v) glycerol and 0.02% (v/v) sodium azide. Primary antibody dilutions used were 1:1000 (anti-T7 mouse monoclonal) and secondary dilutions 1:100 (FITC-conjugated goat anti-mouse; Sigma Immunochemicals). Immunofluorescence was observed and recorded using a Zeiss Axioplan 2 microscope, 63× objective, with a Micro Imager 1400.

Nycodenz density gradients

Nuclear extracts containing ~1.5 mg total protein in a volume of 300 µl were dialysed against Nycodenz (Sigma) gradient low-salt buffer (20 mM Tris-HCl, pH 7.5; 2 mM MgCl₂; 1 mM EDTA) and loaded onto a pre-formed 5 ml gradient of 20–60% Nycodenz dissolved in the above buffer. Samples were spun at 154,000 g for 18 hours at 0°C in a Sorvall AH650 rotor. Gradients were manually fractionated into 18 samples of 250 µl. The density of the samples was determined by measuring the refractive index and applying the formula, density (ρ) in g/cm³=3.242ρ–3.323, where ρ is the refractive index. Proteins were analysed by adding SDS-PAGE buffer directly; the presence of Nycodenz presented no hindrance to pipetting these samples onto SDS-PAGE gels. Fractions were western blotted to detect the T7 tag (mouse monoclonal, Novagen), p116 (rabbit polyclonal, gift of P. Fabrizio), U2AF65 (rabbit polyclonal, gift of R. Davies) and EGR1 (rabbit polyclonal sc-189, Santa Cruz Biotech.). For RNA extraction (see below), samples were precipitated by diluting the Nycodenz fractions threefold with distilled water and adding three volumes of ethanol. They were left overnight at –20°C and spun for 20 minutes at maximum speed on a microfuge.

RNA extraction

RNA lysis buffer, 0.5 ml (4 M guanidine isothiocyanate; 25 mM sodium citrate, pH 7; 1 mM β-mercaptoethanol; 0.5% w/v sodium N-laurylsarcosine; 0.1% v/v Sigma Antifoam A), was added to precipitated samples. Then 50 µl 2 M sodium acetate pH 4 was added, and the sample vortexed. Water-saturated phenol, 0.5 ml, was then added, not pH adjusted, containing 0.1% v/v hydroxyquinoline. Chloroform, 0.2 ml, was added and the sample vortexed. After spinning for 20 minutes at 13,000 rpm in a microfuge at 4°C, 2 volumes of ethanol were added to the water phase, and the sample vortexed. Samples were precipitated overnight at –20°C then spun for 30 minutes at 13,000 rpm in a microfuge. Pellets were washed in 70% ethanol and the pelleted RNA was dissolved in 20–40 µl DEPC-treated water, to which 10 U Superase RNase inhibitor cocktail (Ambion) was added.

Analysis of RNA by RT-PCR and end-labelling

RNA samples (500 ng) were reverse transcribed as per cDNA synthesis kit specifications (Boehringer-Mannheim). cDNA samples were quantified and diluted such that 10 ng template was used in each PCR. Each 30 µl PCR reaction contained 10 pmol of each primer, and was run for 30 cycles (45 seconds at 95°C, 45 seconds at 55°C and 2 minutes at 72°C). Product sizes were compared against DNA markers on 2% agarose gels. The following primers were obtained (Genosys) to amplify WT1 pre-mRNA: forward, 5'-CAGTAGTATCCAGGGTGGTGG-3', derived from the 3' end of mouse intron 9; reverse, 5'-CCGACAGCTGAAGGG-CTTTTCAC-3', 5' end of exon 10, yielding a 380 bp product. For end-labelling, 50–500 ng RNA samples were labelled using T4 RNA ligase (Boehringer Mannheim) and pCp (³²P), using the method of England et al. (England et al., 1980), and separated on a 5% acrylamide/8M urea gel in 1 × TBE buffer (Tris-borate-EDTA).

Oocyte isolation, injection and labelling

Oocytes were isolated from *Xenopus laevis* as described previously (Ryan et al., 1999) and were maintained in OR-2 medium (Evans and Kay, 1991). For microinjection, sets of 20-40 mid-vitellogenic (stage III/IV) oocytes were isolated and 10 nl aliquots containing ~10 pg of purified plasmid DNA were injected, through the animal pole, into the nucleus of each oocyte. RNA was labelled *in vivo* by injecting oocytes with 0.1 μ Ci of [³H]uridine (27 mCi/mmol, Amersham) or with 0.1 μ g of BrUTP (Sigma). Transcription could be inhibited by incubating the oocytes in OR-2 containing 5 μ g/ml actinomycin D. Radioactivity incorporated into RNA was measured after extraction at 60°C with phenol/chloroform buffered to pH 4.2 and precipitation with 2.5 vol ethanol.

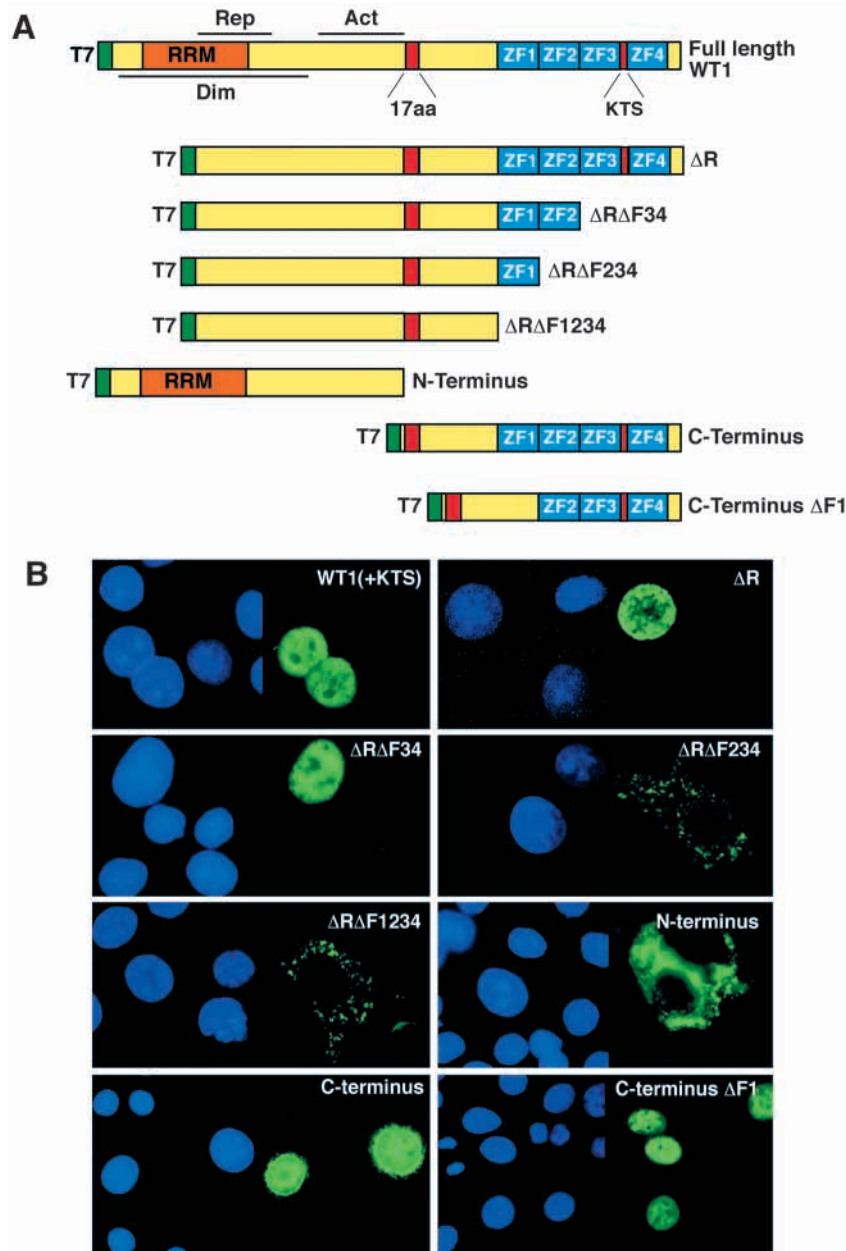
Immunoblotting of oocyte extracts

At 18 or 30 hours after injection, nuclei and cytoplasm were isolated under mineral oil (Sigma) from groups of 20-40 oocytes (Ryan et al.,

1999). Yolk and lipid were extracted from cytoplasm with 1,1,2-trichlorotrifluoroethane (Evans and Kay, 1991) and, after centrifugation at 13,000 rpm for 2 minutes in a microcentrifuge, the clarified supernatant was carefully removed and mixed with an equal volume of SDS-PAGE sample buffer (Sigma). The nuclei were disrupted by sucking up and down through a fine pipette tip before solubilisation in sample buffer. Proteins, equivalent to one cytoplasm or to four nuclei, were separated by SDS-PAGE, transferred to nitrocellulose (Protran, Schleicher and Schull) and immunoblotted as described previously (Ryan et al., 1999). A monoclonal antibody against the T7 epitope (Novagen) and peroxidase-conjugated (HRP) anti-mouse immunoglobulin G (IgG) (Sigma) were both used at a dilution of 1:10,000 and bands were developed using the ECL (Amersham) procedure.

Immunostaining of germinal vesicle spreads

Germinal vesicle (GV) spread preparations from injected oocytes were prepared at 18 or 30 hours post-injection as described (Sommerville et al., 1993). For salt stability studies the preparations were washed sequentially in PBS (Sigma) adjusted to 200, 400 and 600 mM NaCl and stored in 70% ethanol. Before immunostaining, nonspecific binding was blocked by incubating the preparations for 30 minutes in PBS containing 0.05% Tween 20 (PBST) and 10% FCS. Monoclonal anti-T7 epitope (Novagen) and monoclonal anti-bromodeoxyuridine (BrdU) (Sigma) were each used at a dilution of 1:5000 in 10% FCS/PBST, and rabbit polyclonal anti-p116 was used at a dilution of 1:1000. The secondary antibodies were FITC-conjugated goat anti-mouse IgG and TRITC-conjugated goat anti-rabbit IgG (Sigma), both at a dilution of 1:5000 in FCS/PBST. After extensive washing in PBST the preparations were mounted in 50% glycerol, 1 mg/ml *p*-phenylenediamine, pH 8.5, containing 20 ng/ml of 4,6-diamidino-2-phenylindole (DAPI) and viewed using a Leitz Ortholux fluorescence microscope. Images were recorded on Kodak Ektachrome P1600 Professional film.



Immunoprecipitation and salt extraction

Anti-T7 IgG (2 μ l) was linked to 20 μ l of protein A-glass beads (ProSep, Bioprocessing Ltd) as described previously (Ryan et al., 1999). GVs isolated from 50 injected oocytes were needle-sheared in 100 μ l of a solution containing: 100 mM NaCl; 1 mM MgCl₂; 0.1% Nonidet P-40; 20 mM Tris-HCl, pH 7.5 (TBSMN). Extracts were mixed with 5 μ l of the antibody-beads for 60 minutes at 20°C. The beads were washed with TBSMN to remove unbound material and then extracted sequentially with 100 μ l of TBSMN adjusted to 200, 400, 600 and 1000 mM NaCl. Protein from each of the wash fractions was

Fig. 1. Zinc finger two is required for nuclear targeting. (A) Epitope tagged mouse WT1 constructs. Act, activation domain; Dim, dimerisation domain; Rep, repression domain; RRM, putative RNA recognition motif; T7, tag; ZF, zinc finger. Insertions due to alternative splicing: '17 aa' and 'KTS'. (B) Constructs were transiently transfected into Cos7 cells. DAPI stain (left) and corresponding immunofluorescence of tagged protein (right) are shown.

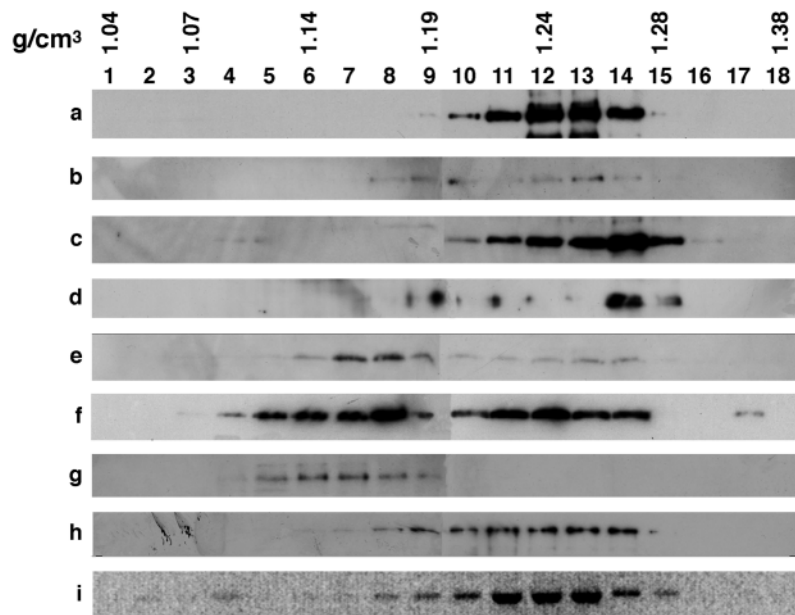


Fig. 2. Zinc finger one is required for co-sedimentation with RNP in mammalian cells. Extracts obtained from transfected Cos7 cells were applied to 20-60% Nycodenz gradients. Western blots: (a) WT1 (+KTS); (b) WT1 (-KTS); (c) $\Delta R\Delta F34$; (d) $\Delta R\Delta F234$; (e) $\Delta R\Delta F1234$; (f) CT $\Delta F1$ (+KTS); (g) native EGR1; (h) U5 snRNP associated splice factor p116; (i) WT1 pre-mRNA (RT-PCR).

precipitated with four volumes of acetone, pelleted, air-dried and immunoblotted.

Anion-exchange chromatography

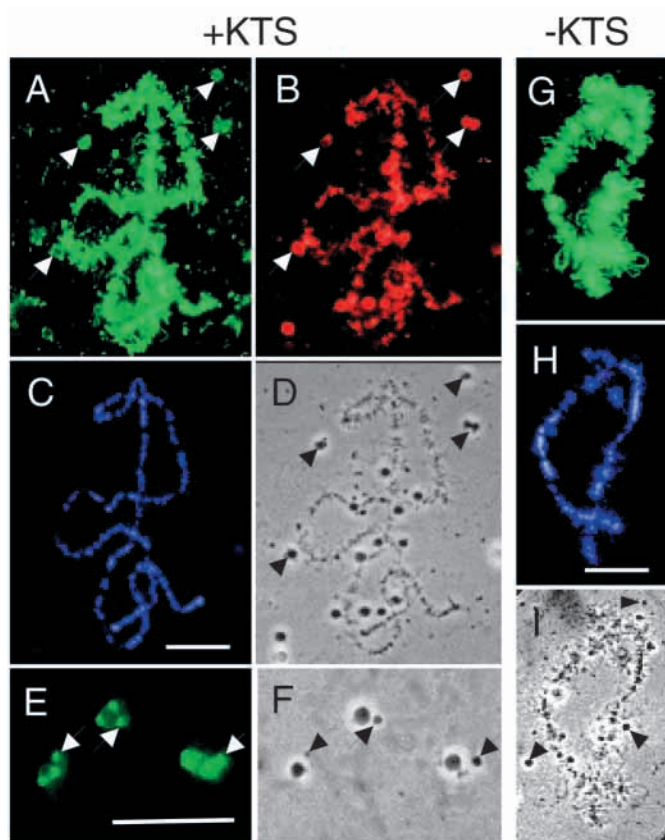
Nuclear extract (1.5 mg) in 2 ml binding buffer (20 mM Tris-HCl, pH 7.5; 50 mM NaCl; 1.5 mM MgCl₂) was applied to a 1 ml Q-Trap anion-exchange column (Amersham Pharmacia Biotech). After reapplying the extract to the column twice, the flow through was

collected, and a salt gradient applied, 100 mM up to 1 M NaCl in 100mM steps, 2 \times 0.5 ml aliquots of buffer at each salt concentration. Samples were precipitated by adding 2 volumes of ethanol, left overnight at -20°C and spun at 13,000 rpm in a microfuge for 30 minutes. One third of each sample was set aside for RNA extraction.

Results

Zinc finger two is required for nuclear targeting

The ability of T7 epitope-tagged constructs to locate to the nucleus was assessed by transient transfection into Cos7 cells, examining >100 transfected cells in each case (Fig. 1). Full-length WT1 (+/-KTS) concentrated in the nucleus. ΔR (deletion of amino acids 1-69, truncating the putative RRM), $\Delta R\Delta F34$ (ΔR minus zinc fingers three and four), C-terminus (CT, amino acids 233-449, +KTS) and CT $\Delta F1$ (CT minus zinc finger one, +KTS) all accumulated in the nucleus, unlike $\Delta R\Delta F234$, $\Delta R\Delta F1234$ or the N-terminus (amino acids 1-235). Similar results were obtained in mouse AC29 cells and human HeLa cells (not shown). We conclude that zinc finger two is required for the nuclear targeting of WT1, which is consistent with previous findings (Bruening et al., 1996).



Co-sedimentation of WT1 with RNP requires zinc finger one

Native WT1 co-sediments with hnRNP proteins and splice factors in high-density fractions (~1.27 g/cm³) in 20-60% Nycodenz gradients (Ladomery et al., 1999). To assess the ability of tagged WT1 to become incorporated into RNP, Cos7 cells were transiently transfected, and extracts prepared 48 hours after transfection were applied to Nycodenz density gradients (Fig. 2). Like native WT1, full-length tagged WT1 (+KTS) peaked in the pre-mRNP range, as did WT1 (-KTS), $\Delta R\Delta F34$, $\Delta R\Delta F234$, the U5 snRNP-associated splice factor

Fig. 3. Localisation of tagged mouse WT1 in nuclear structures of *Xenopus* oocytes. (A-D) Lampbrush chromosome bivalent showing the location of WT1 (+KTS) as FITC image (A), location of p116 as TRITC image (B), corresponding DAPI (C) and phase-contrast (D) images. In addition to locating to the lateral loops of the chromosomes, both WT1 (+KTS) and endogenous p116 locate to Cajal bodies (arrows in A, B and D) and to smaller nuclear particles. (E,F) In images obtained at higher power, WT1 (+KTS) is seen to be specific to the B-snurposomes (arrows) located on the surfaces of the Cajal bodies (E, FITC and F, phase contrast). (G-I) Expression of WT1 (-KTS) shows that it is restricted to the lateral loops of the chromosomes (G) and is not found in Cajal bodies (arrows in I) or in other nuclear particles. The chromosomal DNA axes are stained with DAPI (H).

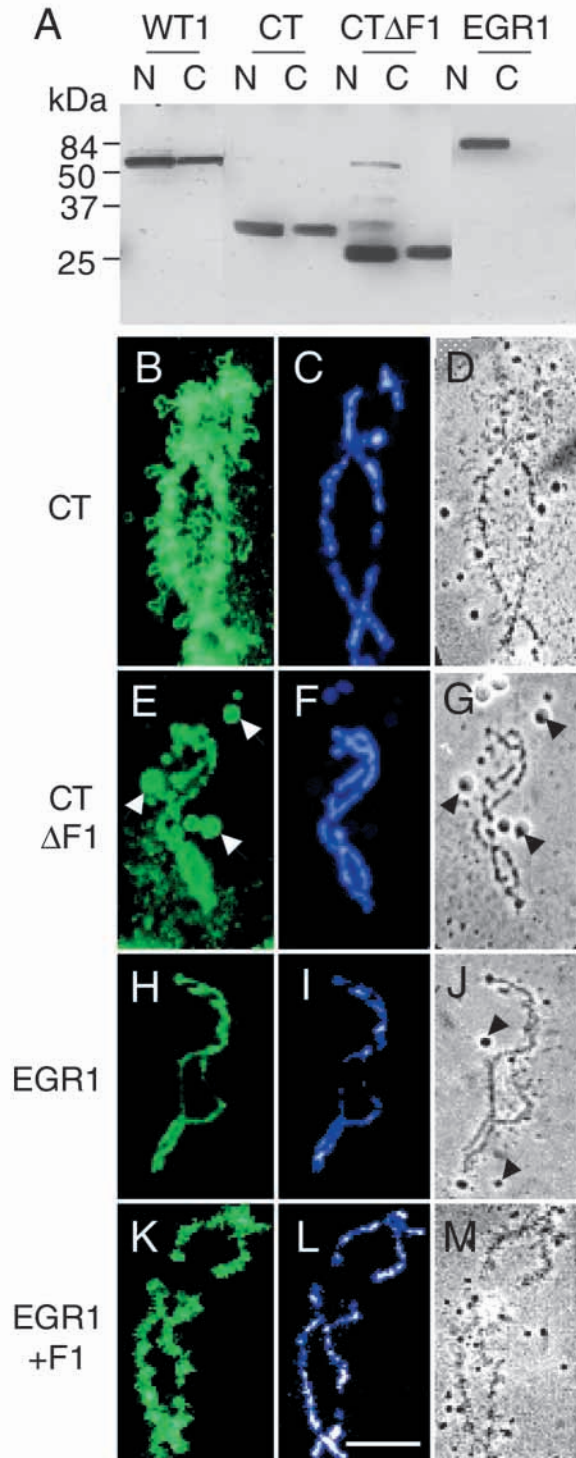


Fig. 4. Nuclear import and localisation of T7-tagged WT1; CT (C-terminus +KTS, amino acids 233-449); CT Δ F1 (+KTS); and EGR1, 18 hours after injecting expression plasmids into the GV of stage IV oocytes. (A) Western blot. Sets of 20 nuclei and cytoplasm were isolated under oil, and protein extracts equivalent to four nuclei (N) and one cytoplasm (C) were loaded. (B-M) Nuclear spreads were immunostained with anti-T7 tag and counterstained with DAPI. Although CT (B-D) immunostained lampbrush chromosome loops similarly to full-length WT1 (Fig. 3), expression of CT Δ F1 appeared to cause chromosome compaction, loop retraction and more intense labelling of Cajal bodies (arrows in E and G). Expression of EGR1 also resulted in chromosome compaction with immunostaining (H) close to the DNA axes (I). As seen in phase contrast (J), lateral loops were less obvious and Cajal bodies (arrows in J) were not immunostained (H). Inclusion of WT1-derived zinc finger one into EGR1 (EGR+F1), however, mimicked full-length WT1 (-KTS) (K-M). Bar, 10 μ m.

Xenopus oocyte nuclear structures, expression plasmids encoding either full-length WT1 (+KTS) or WT1 (-KTS) were injected into the GV of stage IV oocytes, and after 18 hours the GV was isolated and nuclear spreads prepared. The spread preparations were doubly immunostained for WT1 and the splice factor p116 (Fabrizio et al., 1997), and counterstained with DAPI. Both isoforms located to the lateral loops of chromosomes (Fig. 3). However, only the +KTS isoform was detected, along with native p116, on Cajal bodies (Fig. 3A-D). The immunostaining on Cajal bodies was specifically on B-snurposomes, some of which are located on the surfaces of the larger bodies (Fig. 3E-F), with many others scattered free throughout the preparation. The -KTS isoform, although extensively decorating the chromosomal loops, was not seen on Cajal bodies (Fig. 3G-I).

Contribution of zinc finger one to lateral loop and snurposome localizations

We expressed the C-terminus and CT Δ F1 (both +KTS) in oocytes and compared these with expressed EGR1. The deleted forms of WT1 were imported into the nucleus as efficiently as full-length WT1, but the uptake of EGR1 appeared to be more complete after 18 hours (Fig. 4A). On immunostained spread preparations the C-terminus was seen to behave similarly to the full-length protein and located on lateral loops and B-snurposomes (Fig. 4B-D). However, expression of CT Δ F1 caused chromosome compaction, loop retraction and shedding of RNP matrix, with relatively more intense labelling of Cajal bodies (Fig. 4E-G). Similarly, EGR1 expression also appeared to cause chromosome compaction and loop retraction (Fig. 4H-J), although the immunostaining differed in showing no RNP loops; rather, staining was restricted to the chromosomal axes in the pattern similar to that seen with DAPI. Furthermore, EGR1 did not localise to Cajal bodies or in free B-snurposomes. Next, we tested a construct in which WT1 zinc finger one was added to EGR1 upstream of the first zinc finger (EGR1+F1), resembling the zinc finger domain of WT1 (-KTS). Like WT1 (-KTS), EGR1+F1 located to the lateral loops, was not detected on snurposomes, and was not associated with chromosome compaction and loop retraction (Fig. 4K-M).

p116 (Fabrizio et al., 1997) and *WT1* pre-mRNA. By contrast, the closely related transcription factor EGR1 peaked at a lower density (~ 1.15 g/cm³). Δ R Δ F1234 and CT Δ F1 were distributed across the gradient in both lower and higher density fractions. In summary, only constructs that included zinc finger one clearly co-sedimented with pre-mRNP in mammalian cells.

Expression of WT1 (+/-KTS) in *Xenopus* oocytes

To test the ability of T7-tagged mouse WT1 to associate with

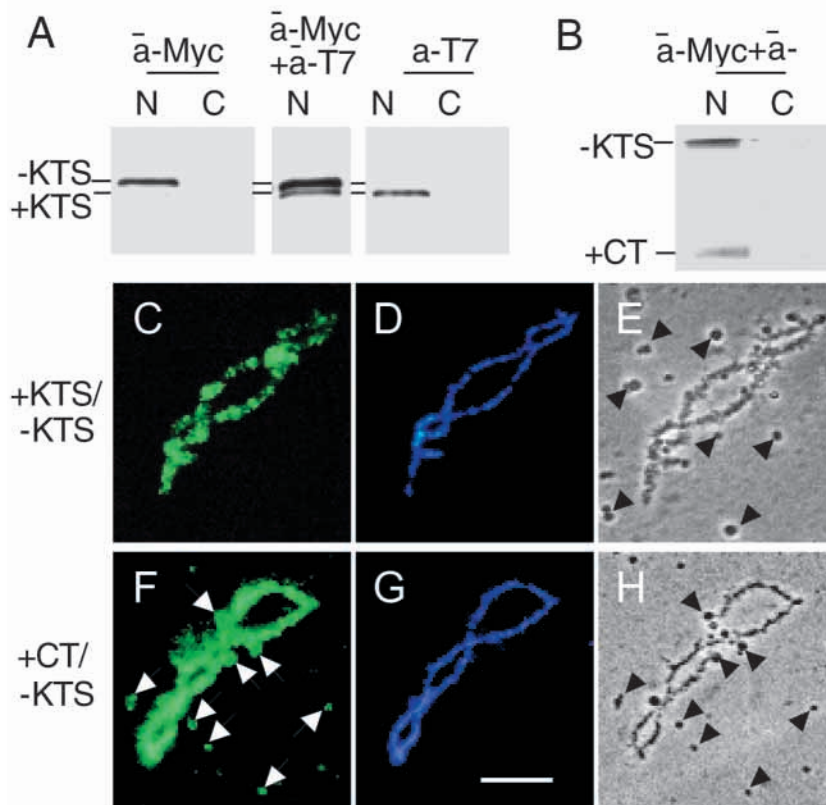


Fig. 5. Nuclear import and localization of co-expressed isoforms: T7-tagged WT1 (+KTS) and Myc-tagged WT1 (-KTS) at 30 hours after plasmid injection. Western blot (A) showing the expression of both full-length constructs, and (B) of full-length Myc-tagged WT1 (-KTS) and T7-tagged CT (C-terminus +KTS). The slower migration of WT1(-KTS) is due to the larger size of the Myc versus the T7 tag. Co-expression of full-length isoforms results in the absence of signal in snurposomes: FITC image detecting the T7 tag (C), corresponding DAPI (D) and phase-contrast (E) images, highlighting Cajal bodies (arrows in E). In contrast, co-expression of only the C-terminus of the +KTS isoform, together with full-length -KTS, results in immunostaining of snurposomes: FITC image detecting the T7-tag (F), corresponding DAPI (G) and phase-contrast (H) images, highlighting B-snurposomes and Cajal bodies (arrows in F and H). Bar, 10 μ m.

The N-terminus can influence localisation of co-expressed isoforms

To check the distribution of full-length WT1 (+/-KTS) WT1 isoforms on co-expression, oocyte nuclei were co-injected with plasmids expressing T7-tagged WT1 (+KTS) and Myc-tagged WT1 (-KTS). At 30 hours post-injection both isoforms had been efficiently imported into the nucleus (Fig. 5A). On examining nuclear spreads, the T7-tag was not seen in snurposome structures (Fig. 5C-E), which were immunostained on expressing the +KTS isoform alone (Fig. 3). This apparent dominance of the -KTS isoform on localisation was ablated on co-expression with CT (C-terminus +KTS) – that is, in the absence of the N-terminus. The CT (+KTS) protein was also efficiently imported into the nucleus (Fig. 5B) and was clearly seen to locate to B-snurposomes on Cajal bodies (Fig. 5F-H).

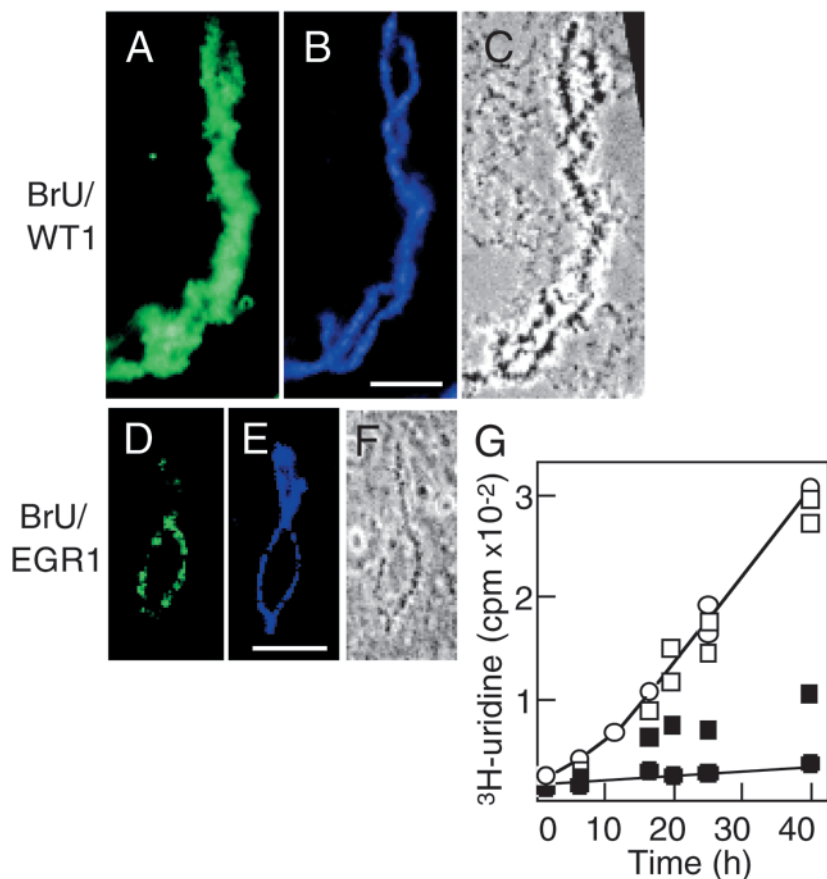


Fig. 6. Effect of the expression of T7-tagged WT1 (-KTS) and EGR1 on transcription from lampbrush chromosomes. For immunostaining, expression plasmids were co-injected with BrUTP (0.1 μ g) or [^3H]-labelled uridine (0.1 μ Ci) into the GV of stage IV oocytes. (A-C) Immunostaining of a chromosome bivalent from oocytes expressing WT1 with anti-BrU showing extensive labelling of lateral loops (A); the DAPI-stained DNA axes (B) and the phase-contrast image (C) are shown. (D-F) Immunostaining of a chromosome bivalent from oocytes expressing EGR1, with anti-BrU showing compacted chromosomes and limited labelling of lateral loops (D). The DAPI-stained DNA axes (E) and the phase-contrast image (F) are also shown. Bar, 10 μ m. (G) Incorporation of [^3H]-labelled uridine into noninjected oocytes (open circles), noninjected oocytes incubated in the presence of 5 μ g/ml actinomycin D (black circles), and oocytes expressing WT1 (open squares) and EGR1 (black squares). Each time-point represents incorporation per oocyte averaged from five oocytes.

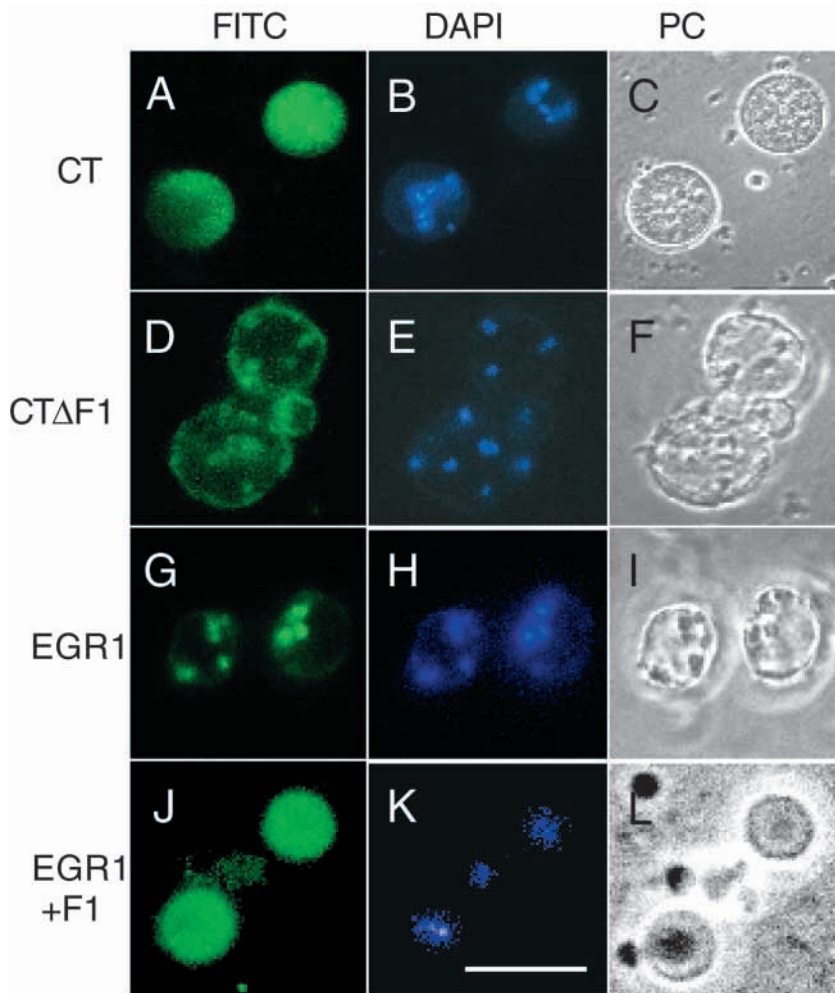


Fig. 7. Localisation of ectopically expressed CT (WT1 C-terminus +KTS), CT Δ F1, EGR1 and EGR1+F1 in the extrachromosomal nucleoli of stage IV oocytes. On expressing the T7-tagged proteins for 30 hours, immunostaining was seen to extend to the nucleoli. Although CT (A-C) and WT1 (not shown) located throughout the nucleolus, CT Δ F1 was more localised to the DNA-containing fibrillar centres as seen in DAPI staining (E). Overexpressed EGR1 gave discrete localisation (G) at the DAPI-stained fibrillar centres (H). By contrast, EGR1+F1 resembled CT (J-L). Bar, 10 μ m.

oocytes for 30 hours resulted in an extension of the immunofluorescence signal to nucleoli. Both full-length WT1 (+KTS) (not shown) and C-terminus (+KTS) were located throughout the nucleolus, including the RNA-rich granular component, but apparently not the DNA-rich fibrillar centres (Fig. 7A-C). By contrast, CT Δ F1 (+KTS) had a more restricted location, primarily to the fibrillar centres (Fig. 7D-F), and EGR1 was seen to be exclusively located to the fibrillar centres (Fig. 7G-I). Strikingly, EGR1+F1 again mimicked the properties of the intact WT1 zinc finger domain and located to the RNA-rich granular component (Fig. 7J-L).

WT1 is stably bound to transcripts

Binding of WT1 zinc fingers to RNA in vitro is salt stable (Zhai et al., 2001). We tested the stability of the interaction of full-length WT1, C-terminus and CT Δ F1 (all +KTS) with transcripts in vivo. Nuclear spreads from oocytes expressing WT1 were washed with increasing concentrations of salt buffer (Fig. 8A-I). At 400 mM and 600 mM NaCl, T7-immunostaining was retained on the lateral loop matrix, albeit in a more compact form (Fig. 8D-I). Chromosome structure was disrupted by washing in 1 M NaCl buffer (not shown).

To obtain a more quantitative estimate of binding stability, we injected the nuclei of sets of 50 oocytes with WT1, C-terminus, CT Δ F1 and co-injected BrUTP. After 18 hours the nuclear contents were needle-sheared and centrifuged, and pellets were resuspended and incubated in the presence of anti-BrU/protein A glass beads. The unbound material was retained and the beads were washed with increasing salt concentrations. The eluted fractions were then precipitated and immunoblotted using anti-T7 tag. Full-length WT1 was the most stably bound protein, eluting only at 1 M NaCl (Fig. 8J). The C-terminus eluted earlier, mainly at 600 mM (Fig. 8K), and CT Δ F1 was the least stably bound, eluting at 400 mM (Fig. 8L). These results confirm the importance of zinc finger one for stable interaction between WT1 and RNP in oocytes, which is consistent with the density gradient data (Fig. 2).

We examined whether native WT1 in mammalian cells is similarly stably associated with transcripts. We applied nuclear extract from AC29 mouse mesothelioma cells to anion exchange resin, which has high affinity for RNA (Palfi et al.,

Effect of expressed WT1 and EGR1 on endogenous transcription rates

Chromosome compaction and loop retraction suggested that EGR1, but notably, not WT1, severely affect transcription rates when overexpressed in oocytes. The effects of WT1 and EGR1 on chromosomal RNA transcription could be compared directly by labelling injected oocytes with BrUTP. In oocytes expressing WT1 (-KTS), immunostaining of incorporated BrU was seen to be extensive over the lateral loops (Fig. 6A-C). By contrast, chromosomes isolated from oocytes expressing EGR1 were poorly labelled with BrUTP, with immunostaining occurring at relatively few loci (Fig. 6D-F). Transcription rates were then checked by the incorporation of [3 H]-labelled uridine into transcripts. Rates of incorporation in oocytes expressing WT1 were found to be similar to rates in noninjected oocytes (Fig. 6G). By contrast, transcription in oocytes expressing EGR1 was severely reduced. After about 10 hours from EGR1 plasmid injection, the incorporation rate was little more than the rate obtained with oocytes treated with actinomycin D, a potent inhibitor of transcription (Fig. 6G).

Nucleolar localisation of WT1 and EGR1

We also observed that the expression of tagged proteins in

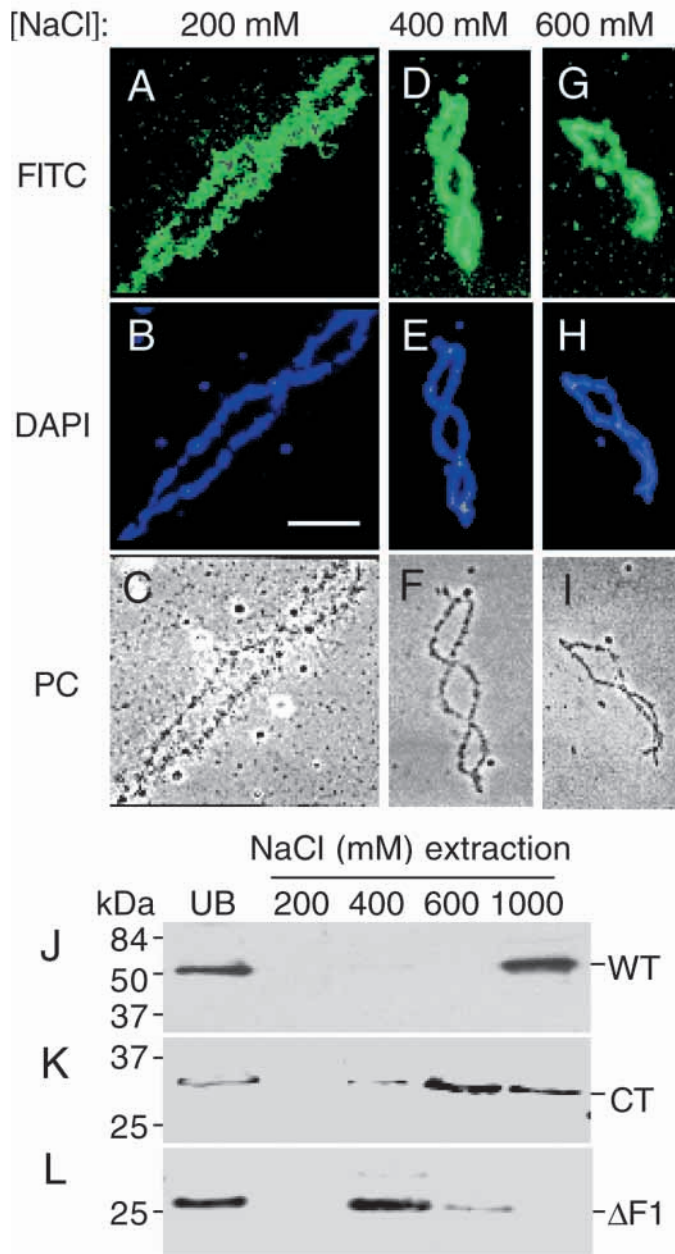


Fig. 8. Stability of interaction of WT1, CT and CTΔF1 with the nascent RNA transcripts of lampbrush chromosomes. Isolated nuclei were spread and washed extensively in solutions containing 200 mM, 400 mM and 600 mM NaCl. Although the chromosomes became more condensed in the higher salt conditions, most of the anti-T7 signal on the loop matrix (A,D,G) was retained, albeit in a more compact form. The corresponding DAPI (B,E,H) and phase-contrast (C,F,I) images are shown. Bar, 10 μ m. (J,K,L) Salt stability of RNP immunoprecipitated from oocytes expressing WT1, CT and CTΔF1 (see text for details).

1989). After collecting the flow through, a series of salt washes was applied, increasing from 100 mM to 1 M NaCl (Fig. 9). The majority of bound nuclear proteins eluted in the 300–500 mM range. By contrast, native WT1 eluted in the 1 M NaCl wash together with the bulk of snRNA and pre-mRNA, consistent with results using *Xenopus* oocyte (Fig. 8).

Discussion

The *WT1* gene encodes a multifunctional transcription factor that has a role in development and disease. However, evidence suggests that, in addition to its ability to bind DNA and regulate the transcription of key target genes, WT1 has an additional role in post-transcriptional processes. The aim of this study was to obtain evidence that WT1 interacts with transcripts and splice factors *in vivo*. On the basis of previous findings, we focused on the role of zinc finger one and the +/–KTS alternative splice (Larsson et al., 1995; Caricasole et al., 1996; Bardeesy and Pelletier, 1998; Davies et al., 1998; Zhai et al., 2001). Our approach was to express epitope-tagged constructs in mammalian cells and *Xenopus* oocytes. *Xenopus* oocytes are well suited for studying the biochemical properties and nuclear localisations of both native and tagged proteins and their domains (Bellini et al., 1995; Ryan et al., 1999; Ladomery et al., 2000; Smillie and Sommerville, 2002). In particular, germinal vesicles (oocyte nuclei) have the following advantages: a high concentration of the components of the RNA synthesis and processing machinery, together with the ability to make nuclear spread preparations and to discriminate individual nuclear structures at high resolution. The latter include the lampbrush chromosome loops, highly active in pol II and III transcription; chromomeres, containing silenced genes and condensed chromatin; Cajal bodies (previously known as spheres, or coiled bodies), which are sites of assembly of pol II, II, III transcriptosomes and spliceosomes; B-snurposomes, which transport pol II transcriptosomes and spliceosomes from Cajal bodies to loops; and extrachromosomal nucleoli (Gall et al., 1999).

We previously reported that T7-tagged WT1 (+KTS) colocalises with the essential splice factor p116 in nuclear speckles in both HeLa and Cos7 cells, and that the C-terminus but not the N-terminus of WT1 associates with nuclear poly(A)⁺ RNP (Ladomery et al., 1999). We prepared additional constructs, which included a truncation of the putative RRM and deletions of zinc fingers. We began by testing the ability of the new constructs to target to the nucleus. In a previous study of WT1 nuclear localisation signals, fusion of zinc fingers two and three with β -galactosidase resulted in nuclear targeting (Bruening et al., 1996). We confirm the importance of zinc finger two for nuclear targeting. The reason for its importance is the high proportion of basic amino acids in zinc finger two, resembling a nuclear localisation signal. The ability of zinc fingers to direct nuclear targeting is not unique to WT1. For example, zinc fingers two and three are required for nuclear targeting of EGR1 (Gashler et al., 1993). Next, we transiently transfected Cos7 cells with the above constructs and ran soluble extract on Nycodenz density gradients. Native WT1 present in mouse cell lines and fetal kidneys co-sediments with RNP on Nycodenz (Ladomery et al., 1999). We found that both (+ and –KTS) isoforms of expressed WT1 co-sedimented with splice factors and pre-mRNA, unlike EGR1. Constructs that retained zinc finger one similarly peaked in the pre-mRNP range.

In *Xenopus* oocytes we observed an accumulation of both +/–KTS isoforms of WT1 on the lateral loops of lampbrush chromosomes, indicating their ability to bind nascent transcripts. By stark contrast, the transcription factor EGR1 located to the chromosomal axes and binding was associated with loop retraction and transcriptional shut-down. Notably,

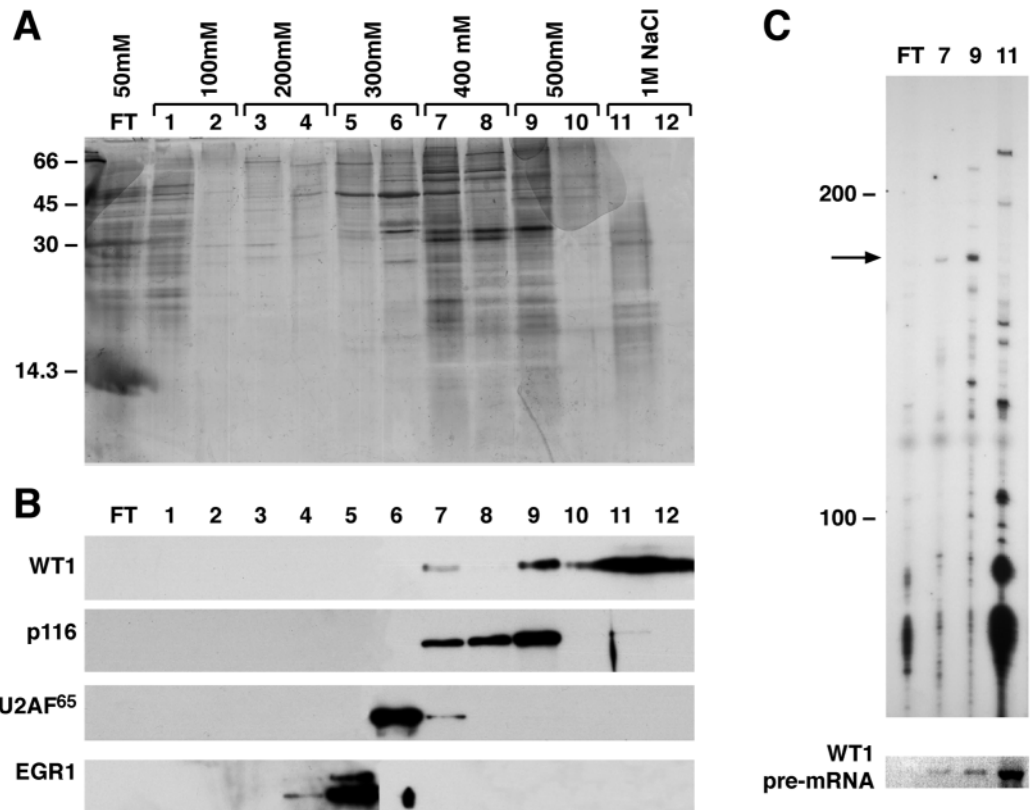


Fig. 9. Nuclear extract from AC29 mouse mesothelioma cells was applied to anion exchange and a salt wash gradient applied. (A) Protein stain, showing flow through (FT) and increasing salt elutions. (B) Western blot showing the distribution of native WT1, the splice factors p116 and U2AF65, and EGR1. (C) Presence of RNA in fractions FT, 7, 9 and 11. Small nuclear RNA species, end-labelled by T4 RNA ligase, are shown above. The arrow points to U1 snRNA. WT1 pre-mRNA is shown below (RT-PCR).

WT1 (+KTS) accumulated in B-snurposomes. These are 20-30 nm particles corresponding to the components of the interchromatin granules of somatic nuclei described as 'transcriptosomes' (Gall et al., 1999). Transcriptosomes are sites of storage for the machinery required for transcription and RNA processing. These results agree with previous studies in which WT1 (+KTS) was found to colocalise with splice factors in nuclear speckles in mammalian cells (Larsson et al., 1995) and to interact with the splice factor U2AF65 (Davies et al., 1998). More recently, Hammes and colleagues (Hammes et al., 2001) reported that an isoform-specific mouse knockout in which only the +KTS isoform is produced resulted in more prominent nuclear speckle localisation. We also found that CTΔF1 (+KTS) accumulated in B-snurposomes even more prominently than full-length protein. This is consistent with the apparent ability of zinc fingers 2-4 (+KTS) to interact with U2AF65, independently of zinc finger one, in the yeast two-hybrid assay (Davies et al., 1998). It is tempting to speculate that the localisation of WT1 (+KTS) on snurposomes may depend on its interaction with endogenous *Xenopus* U2AF65. The absence of zinc finger one could make more protein available for U2AF65, as opposed to transcripts.

The interaction between the +KTS and -KTS isoforms in vivo is poorly understood. Strikingly, co-expression of both tagged WT1 isoforms in oocytes impaired the accumulation of +KTS protein in snurposomes, as long as the N-terminus was present. Significantly, WT1 is reported to dimerise via its N-terminus (Moffett et al., 1995). We speculate that WT1 (-KTS) titrates WT1 (+KTS) away from snurposomes. These observations provide evidence that +/-KTS isoforms, whose intracellular ratio is crucial in development, dimerise in vivo.

To our surprise, expressed EGR1 caused loop retraction and

chromosome compaction. However, this may be explained by a generic interaction with DNA and/or chromatin. We also found that CTΔF1 (+KTS) caused loop retraction, although not as clearly as EGR1. This was not the case for full-length WT1 (-KTS) which, similarly overexpressed, did not interfere with normal transcription rates. We speculate that by associating

WT1-ZF1	P FMCAYPG CNK R Y FKLSHL Q MHSRKH T G E K
SP1-ZF1	QHICHIQGGCKVYGKTSHLRAHLRWHTGER
SP3-ZF1	QHICHIQGGCKVYGKTSHLRAHLRWHSGER
MGIF-ZF1	SHICSHPGCGKTYFKSSHLKAHVTRHTG E K
GKLF-ZF1	THTCDYAGCGKTYTKSSHLKAHLRHTHTG E K
KLF2-ZF1	THTCSYTNCGKTYTKSSHLKAHLRHTHTG E K
WT1-ZF2	PYQCDFKDCERRF S RS D QLKR H QR R HTG V K
EGR1-ZF1	PYACPVESCDRRF S RS D ELTRH I R I HTG Q K
SP1-ZF2	PFMCNWSYCGK R FR S DELQ R HR K RHTG E K
SP3-ZF2	PFICNWMF C GK R FR S DELQ R HR R RHTG E K
MGIF-ZF2	PFSCSWKGCERRF A RS D ELSR H RR T HTG E K
GKLF-ZF2	PYHCDWDGCGW K F A RS D ELTR H YR K HTG H R
KLF2-ZF2	PYHCNWE G CGW K F A RS D ELTR H YR K HTG H R
WT1-ZF3	PFQCKT-- C Q R K F RS D HL K TH T R T HTG E K
EGR1-ZF2	PFQCR I -- C M R N F RS D HL T H I R T HTG E K
SP1-ZF3	KFAC P E-- C P K R F MR S DL S K H I K TH Q N K K
SP3-ZF3	KFV C P E -- C S K R F MR S DL L A K H I K T H Q N K K
MGIF-ZF3	KFAC P M-- C DR R F M RS D HL T K H ARR H LS A K
GKLF-ZF3	PFQ C Q K -- C D R A F RS D HL A L H M K R H F---
KLF2-ZF3	PFQ C H L -- C D R A F RS D HL A L H M K R H M---
WT1-ZF4	PFSCR W HS C Q K FK A RS D EL V R H H N M-- H Q R N...
EGR1-ZF3	PFAC D I-- C G R K F AR S DER K R H T K I-- H L R Q

Fig. 10. Comparison of zinc fingers in mouse WT1 and other transcription factors with closely related Krüppel class zinc fingers. Note that WT1 has four zinc fingers, whereas the others have three. WT1 zinc fingers 1-3 align with corresponding zinc fingers in SP1, SP3, MGIF, GKLF and KLF2. EGR1 zinc fingers align with WT1 zinc fingers 2-4. WT1 zinc finger one has distinct amino acids (shown in bold).

with nascent transcripts, expressed WT1 is unable to interfere with the transcriptional machinery. Interestingly, the inclusion of WT1 zinc finger one in EGR1 impaired loop retraction. This suggests that EGR1+F1 has acquired the ability to interact with RNA. We also observed full-length WT1 (+KTS) and C-terminus (+KTS) in the RNA-rich granular component of nucleoli. By contrast, CTAF1 (+KTS) and EGR1 accumulated in central foci that stain with DAPI and correspond to the DNA-rich fibrillar centres. As before, the inclusion of WT1 zinc finger one in EGR1 gave rise to a protein with properties similar to WT1 (-KTS). Future work will address whether or not native WT1 passes through nucleoli.

All of the above was consistent with the ability of WT1 to bind to RNA in vitro, in a salt-stable manner (Zhai et al., 2001). To test the stability of the association between WT1 and nascent transcripts, we washed lampbrush chromosome spreads in high salt buffer. This treatment did not remove WT1 from the chromosomes. Full-length WT1 in immunoprecipitated RNP was also stably bound, in contrast to CTAF1, which again points to a central role for zinc finger one. However, WT1 was more stably bound than the C-terminus alone, suggesting that additional domains in the N-terminus may contribute to RNA binding – for example, the putative RRM or dimerisation domains in the N-terminus. It is also likely that other zinc fingers contribute to RNA binding in vivo as they do in vitro. Zinc finger proteins that bind to RNA generally use multiple zinc fingers. To relate these findings to native WT1, we fractionated nuclear extract obtained from mouse mesothelioma cells on anion exchange resin. WT1 clearly co-eluted with snRNAs and pre-mRNA in anion exchange in a high-salt wash, consistent with results obtained with *Xenopus* oocyte.

In summary, we present evidence that both isoforms (+/-KTS) of WT1 bind to transcripts in vivo and that zinc finger one has a crucial role to play in RNA binding. Only WT1 (+KTS) was detected in *Xenopus* oocyte B-snurposomes, both free and on Cajal bodies, which is consistent with an interaction of WT1 (+KTS) with endogenous splice factors. That WT1 (-KTS) also interacts with transcripts is corroborated by its sedimentation properties on density gradients, accumulation on lateral loops (this study) and ability to bind to RNA in vitro (Caricasole et al., 1996; Bardeesy and Pelletier, 1998; Zhai et al., 2001). By contrast, the related transcription factor EGR1, which lacks the equivalent of WT1 zinc finger one, behaved differently. We suggest that during evolution, WT1 has acquired the ability to influence gene expression at the post-transcriptional level, thanks to the properties of zinc finger one and the +KTS alternative splice. The +KTS alternative splice is unique to WT1 in the EGR family of transcription factors. However, the question arises as to what is particular about WT1 zinc finger one. Unlike EGR1, other related transcription factors possess the equivalent of zinc finger one. An alignment between zinc finger domains of WT1, EGR1 and other related proteins suggests that WT1 zinc finger one has at least seven distinct amino acids, and it is tempting to speculate that these differences relate to the ability of zinc finger one to bind RNA (Fig. 10).

WT1 is not unique in its ability to interact both with DNA and RNA. There are now many examples of such multifunctional proteins, and many of these are zinc-finger proteins (Ladomery, 1997; Wilkinson and Shyu, 2001; Ladomery and Delleire, 2002). The priority now is to search

for in vivo RNA targets and the role of WT1 in post-transcriptional gene regulation. Future studies will also focus on the molecular basis of WT1: RNA interactions, a possible link between DNA and RNA targets, and their connection to pathways involved in development and disease.

This work was supported by the Medical Research Council UK. We are grateful to P. Fabrizio and R. Davies for the gift of antibodies.

References

- Barboux, S., Niaudet, P., Gubler, M. C., Grunfeld, J. P., Jaubert, F., Kuttann, F., Fekete, C. N., Souleyreau-Therville, N., Thibaud, E., Fellous, M. et al. (1997). Donor splice-site mutations in WT1 are responsible for Frasier syndrome. *Nat. Genet.* **17**, 467-470.
- Bardeesy, N. and Pelletier, J. (1998). Overlapping RNA and DNA binding domains of the WT1 tumor suppressor gene product. *Nucleic Acids Res.* **26**, 1784-1792.
- Bellini, M., Lacroix, J. C. and Gall, J. G. (1995). A zinc-binding domain is required for targeting the maternal nuclear protein PwA33 to lampbrush chromosome loops. *J. Cell Biol.* **131**, 563-570.
- Bruening, W., Moffett, P., Chia, S., Heinrich, G. and Pelletier, J. (1996). Identification of nuclear localization signals within the zinc fingers of the WT1 tumor suppressor gene product. *FEBS Lett.* **393**, 41-47.
- Call, K., Glaser, T., Ito, C. Y., Buckler, A. J., Pelletier, J., Haber, D. A., Rose, E. A., Kral, A., Yeager, H. and Lewis, W. H. (1990). Isolation and characterization of a zinc finger polypeptide gene at the human chromosome 11 Wilms' tumor locus. *Cell* **60**, 509-520.
- Caricasole, A., Duarte, A., Larsson, S. H., Hastie, N. D., Little, M., Holmes, G., Todorov, I. and Ward, A. (1996). RNA binding by the Wilms' tumor suppressor zinc finger proteins. *Proc. Natl. Acad. Sci. USA* **93**, 7562-7566.
- Davies, R. C., Calvio, C., Bratt, E., Larsson, S. H., Lamond, A. I. and Hastie, N. D. (1998). WT1 interacts with the splicing factor U2AF65 in an isoform-dependent manner and can be incorporated into spliceosomes. *Genes Dev.* **12**, 3217-3225.
- Davis, M. R., Manning, L. S., Whitaker, M. J., Garlepp, M. J. and Robinson, B. W. S. (1992). Establishment of a murine model of malignant mesothelioma. *Int. J. Cancer* **52**, 881-886.
- England, T. E., Bruce, A. G. and Uhlenbeck, O. C. (1980). Specific labeling of 3' termini of RNA with T4 RNA ligase. *Methods Enzymol.* **65**, 65-74.
- Evans, J. P. and Kay, B. K. (1991). Biochemical fractionation of oocytes. *Methods Cell Biol.* **36**, 133-148.
- Fabrizio, P., Lagerbauer, B., Lauber, J., Lane, W. S. and Luhrmann, R. (1997). An evolutionarily conserved U5 snRNP-specific protein is a GTP-binding factor closely related to the ribosomal translocase EF-2. *EMBO J.* **16**, 4092-4106.
- Gall, J. G., Bellini, M., Wu, Z. and Murphy, C. (1999). Assembly of the nuclear transcription and processing machinery: Cajal bodies (coiled bodies) and transcriptosomes. *Mol. Biol. Cell* **10**, 4385-4402.
- Gashler, A. L., Swaminathan, S. and Sukhatme, V. P. (1993). A novel repression module, an extensive activation domain, and a bipartite nuclear localisation signal defined in the immediate-early transcription factor Egr-1. *Mol. Cell. Biol.* **13**, 4556-4571.
- Gessler, M., Konig, A., Arden, K., Grundy, P., Orkin, S., Sallan, S., Peters, C., Ruyle, S., Mandell, J. and Li, F. (1994). Infrequent mutation of the WT1 gene in 77 Wilms' Tumors. *Hum. Mutat.* **3**, 212-222.
- Hammes, A., Guo, J. K., Lutsch, G., Leheste, J. R., Landrock, D., Ziegler, U., Gubler, M. C. and Schedl, A. (2001). Two splice variants of the Wilms' tumour 1 gene have distinct functions during sex determination and nephron formation. *Cell* **106**, 319-329.
- Hastie, N. D. (2001). Life, sex, and wt1 isoforms- three amino acids can make all the difference. *Cell* **106**, 391-394.
- Kennedy, D., Ramsdale, T., Mattick, J. and Little, M. (1996). An RNA recognition motif in Wilms' tumour protein (WT1) revealed by structural modelling. *Nat. Genet.* **12**, 329-331.
- King-Underwood, L. and Pritchard-Jones, K. (1998). Wilms' tumor (WT1) gene mutations occur mainly in acute myeloid leukemia and may confer drug resistance. *Blood* **91**, 2961-2968.
- Klamt, B., Koziell, A., Poulat, F., Wieacker, P., Scambler, P., Berta, P. and Gessler, M. (1998). Frasier syndrome is caused by defective alternative splicing of WT1 leading to an altered ratio of WT1 +/-KTS splice isoforms. *Hum. Mol. Genet.* **7**, 709-701.

- Ladomery, M. (1997). Multifunctional proteins suggest connections between transcriptional and post-transcriptional processes. *BioEssays* **19**, 903-909.
- Ladomery, M. and Dellaire, G. (2002). Multifunctional zinc finger proteins in development and disease. *Ann. Hum. Genet.* **66**, 331-342.
- Ladomery, M., Slight, J., McGhee, S. and Hastie, N. D. (1999). Presence of WT1, the Wilms' tumour suppressor gene product, in nuclear poly(A)⁺ RNP. *J. Biol. Chem.* **274**, 36520-36526.
- Ladomery, M., Marshall, R., Arif, L. and Sommerville, J. (2000). C4SR, a novel zinc finger protein with SR-repeats, is expressed during early development of *Xenopus*. *Gene* **256**, 293-302.
- Laity, J. H., Chung, J., Dyson, H. J. and Wright, P. E. (2000a). Alternative splicing of Wilms' tumor suppressor protein modulates DNA binding activity through isoform-specific DNA-induced conformational changes. *Biochemistry* **39**, 5341-5348.
- Laity, J. H., Dyson, H. J. and Wright, P. E. (2000b). DNA-induced alpha-helix capping in conserved linker sequences is a determinant of binding affinity in Cys(2)-His(2) zinc fingers. *J. Mol. Biol.* **295**, 719-727.
- Laity, J. H., Dyson, H. J. and Wright, P. E. (2000c). Molecular basis for modulation of biological function by alternate splicing of the Wilms' tumor suppressor protein. *Proc. Natl. Acad. Sci. USA* **97**, 11932-11935.
- Larsson, S. H., Charlieu, J. P., Miyagawa, K., Engelkamp, D., Rassoulzadegan, M., Ross, A., Cuzin, F., van Heyningen, V. and Hastie, N. D. (1995). Subnuclear localization of WT1 in splicing or transcription factor domains is regulated by alternative splicing. *Cell* **81**, 391-401.
- Lee, S. B., Huang, K., Palmer, R., Truong, V. B., Herzlinger, D., Kolquist, K. A., Wong, J., Paulding, C., Yoon, S. K., Gerald, W. et al. (1999). The Wilms tumor suppressor WT1 encodes a transcriptional activator of amphiregulin. *Cell* **98**, 663-673.
- Little, M., Holmes, G. and Walsh, P. (1999). WT1: what has the last decade told us? *BioEssays* **21**, 191-202.
- Little, N. A., Hastie, N. D. and Davies, R. C. (2000). Identification of WTAP, a novel Wilms' tumour 1-associating protein. *Hum. Mol. Genet.* **9**, 2231-2239.
- Mayo, M. W., Wang, C. Y., Drouin, S. S., Madrid, L. V., Marshall, A. F., Reed, J. C., Weissman, B. E. and Baldwin, A. S. (1999). WT1 modulates apoptosis by transcriptionally upregulating the bcl-2 proto-oncogene. *EMBO J.* **18**, 3990-4003.
- Moffett, P., Bruening, W., Nakagama, H., Bardeesy, N., Housman, D., Housman, D. E. and Pelletier, J. (1995). Antagonism of WT1 activity by protein self-association. *Proc. Natl. Acad. Sci. USA* **92**, 11105-11109.
- Nachtigal, M. W., Hirokawa, Y., Enyeart-VanHouten, D. L., Flanagan, J. N., Hammer, G. D. and Ingraham, H. A. (1998). Wilms' tumor 1 and Dax-1 modulate the orphan nuclear receptor SF-1 in sex-specific gene expression. *Cell* **93**, 445-454.
- Palfi, Z., Bach, M., Solymosy, F. and Lührmann, R. (1989). Purification of the major UsnRNPs from broad bean nuclear extracts and characterization of their protein constituents. *Nucleic Acids Res.* **17**, 1445-1458.
- Penalva, L. O., Ruiz, M. F., Ortega, A., Granadino, B., Vicente, L., Segarra, C., Valcarcel, J. and Sanchez, L. (2000). The *Drosophila* fl(2)d gene, required for female-specific splicing of Sxl and tra pre-mRNAs, encodes a novel nuclear protein with a HQ-rich domain. *Genetics* **155**, 129-139.
- Ryan, J., Llinas, A. J., White, D. A., Turner, B. M. and Sommerville, J. (1999). Maternal histone deacetylase is accumulated in the nuclei of *Xenopus* oocytes as protein complexes with potential enzyme activity. *J. Cell Sci.* **112**, 2441-2452.
- Smillie, D. A. and Sommerville, J. (2002). RNA helicase p54 (DDX6) is a shuttling protein involved in nuclear assembly of stored mRNP particles. *J. Cell Sci.* **115**, 395-407.
- Sommerville, J., Baird, J. and Turner, B. M. (1993). Histone H4 acetylation and transcription in amphibian oocytes. *J. Cell Biol.* **120**, 277-290.
- Werner, H., Rauscher, F. J., III, Sukhatme, V. P., Drummond, I. A., Roberts, C. T., Jr and LeRoith, D. (1994). Transcriptional repression of the insulin-like growth factor I receptor (IGF-I-R) gene by the tumor suppressor WT1 involves binding to sequences both upstream and downstream of the IGF-I-R gene transcription start site. *J. Biol. Chem.* **269**, 12577-12582.
- Wilhelm, D. and Englert, C. (2002). The Wilms tumor suppressor WT1 regulates early gonad development by activation of Sf1. *Genes Dev.* **16**, 1839-1851.
- Wilkinson, M. F. and Shyu, A. B. (2001). Multifunctional regulatory proteins that control gene expression in both the nucleus and the cytoplasm. *BioEssays* **23**, 775-787.
- Zhai, G., Iskandar, M., Barilla, K. and Romaniuk, P. J. (2001). Characterization of RNA aptamer binding by the Wilms' tumor suppressor protein WT1. *Biochemistry* **40**, 2032-2040.